Electronic Supplementary Material (ESI) for RSC Advances.
This journal is © The Royal Society of Chemistry 2017

Supplementary Information

Tunable Ag@SiO_2 core-shell nanocomposites for broad spectrum antibacterial applications

Mark A. Isaacs,[a] Lee J. Durndell[a], Anthony C Hilton[b], Luca Olivi[c], Christopher M. A. Parlett[a], Karen Wilson[a] and Adam F. Lee[a]

[a]*European Bioenergy Research Institute, Aston University, Birmingham, B4 7ET.*
[b]*Life and Health Sciences, Aston University, Birmingham, B4 7ET..*
[c]*Sincotrone Trieste, 34149 Basovizza, Trieste, Italy.*

Nanocomposite synthesis

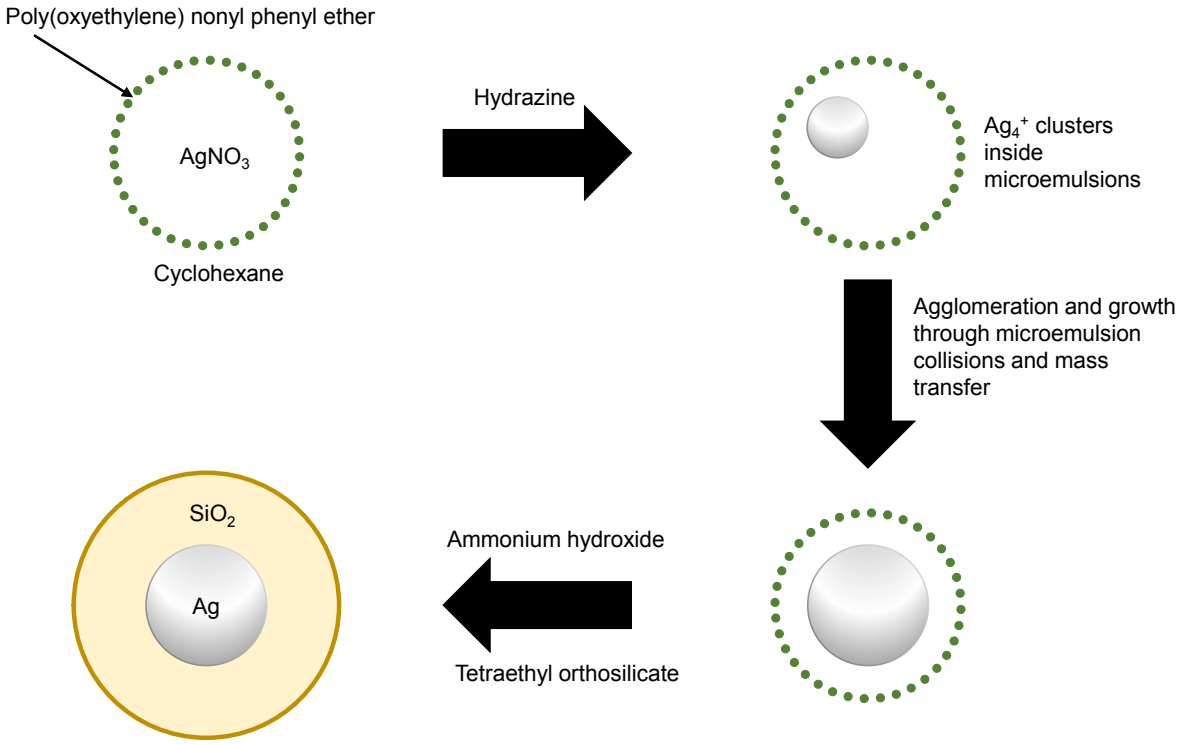

Fig. S1: Reverse microemulsion synthesis of Ag@SiO_2 nanocomposites.

Table S1. Ion concentrations in SBF solution

Ion	Simulated Body Fluid / mM	Blood Plasma / mM
Na^+	142	142
K^+	5	5
Mg^{2+}	1.5	1.5
Ca^{2+}	2.5	2.5
Cl^-	148.8	103
HCO_3^-	4.2	27
HPO_4^{2-}	1	1
SO_4^{2-}	0.5	0.5

Nanocomposite characterisation

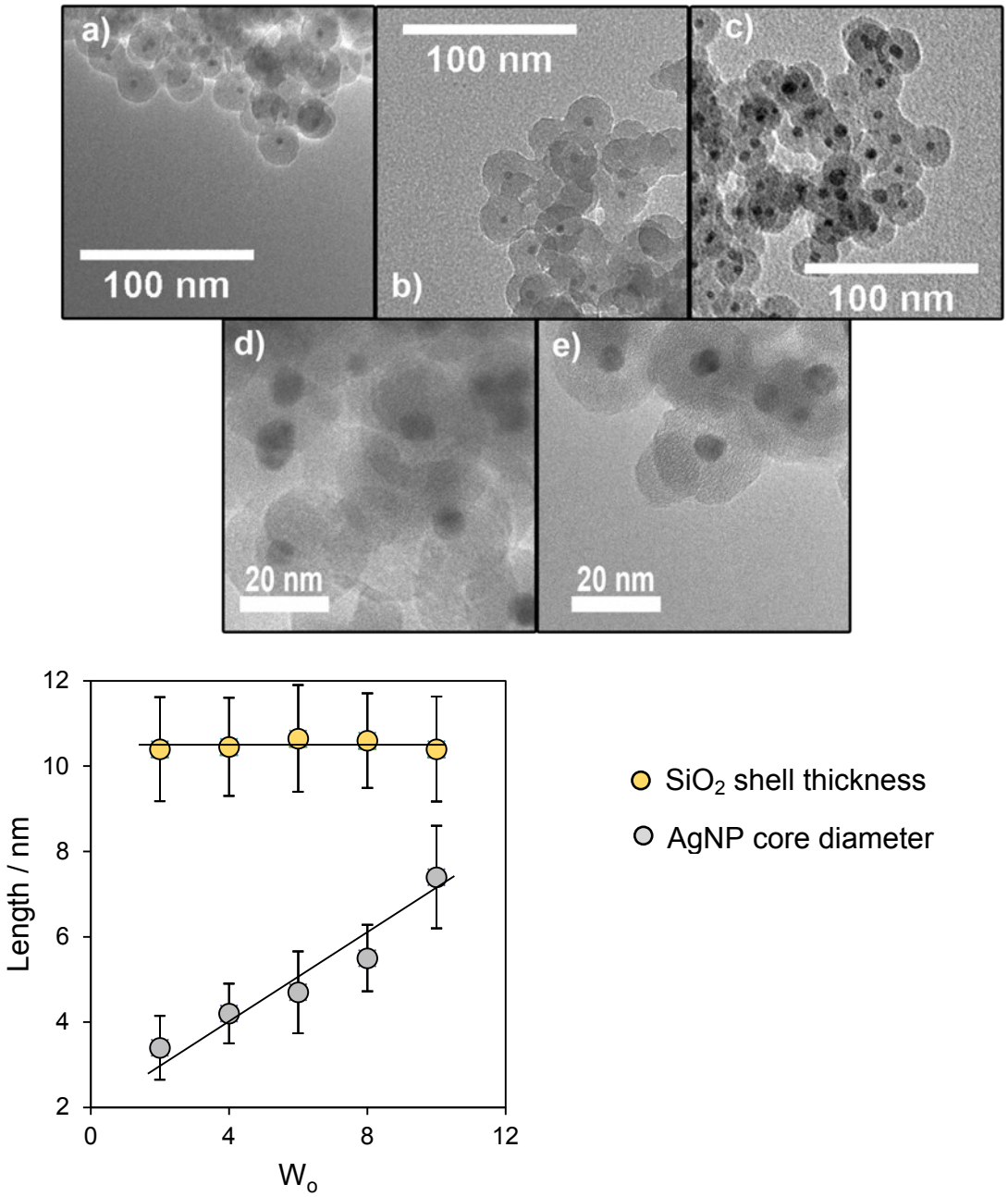

Fig. S2. Representative HRTEM images of Ag@SiO_2 core-shell nanocomposites with a H value of 100 and W_o values of a) 2, b) 4, c) 6, d) 8 and e) 10. (Bottom) Average AgNP particle sizes and SiO_2 shell thicknesses from HRTEM analysis images of Ag@SiO_2 core-shell nanocomposites with a H value of 130 as a function of W_o.

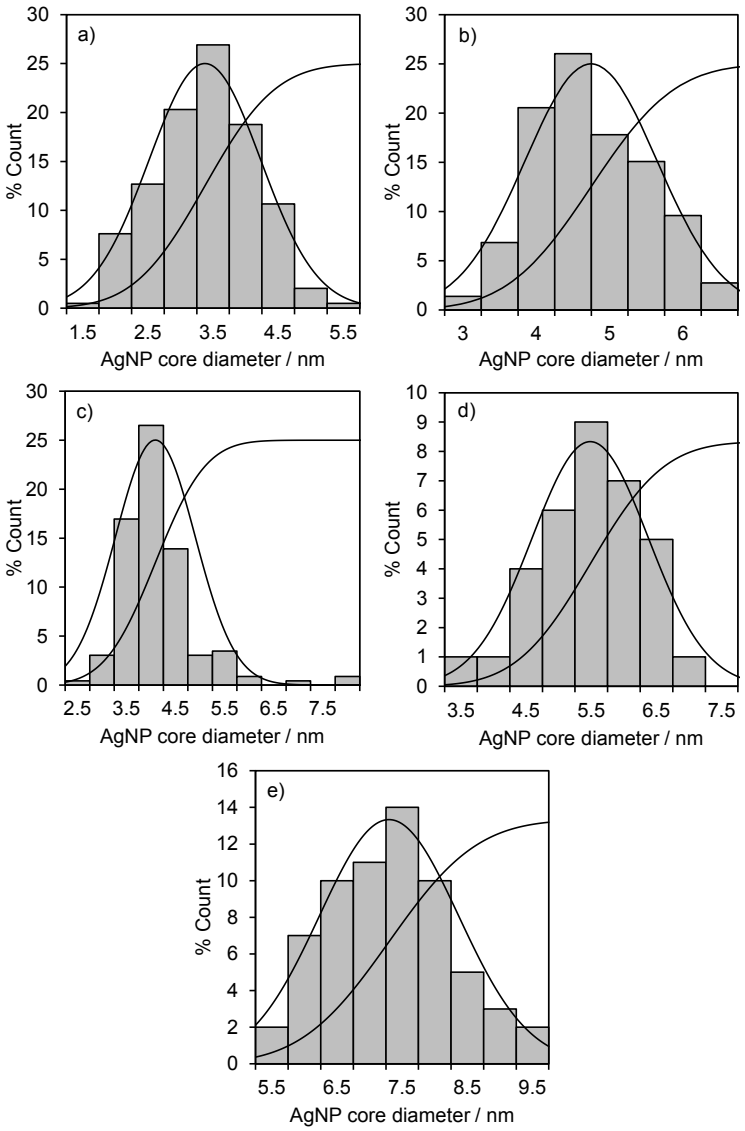

Fig. S3. Silver core size distributions, normal and cumulative size distributions of $Ag@SiO_2$ core-shell nanocomposites determined by HRTEM for a H value of 130 and W_o ratios of a) 2, b) 4, c) 6, d) 8 and e) 10.

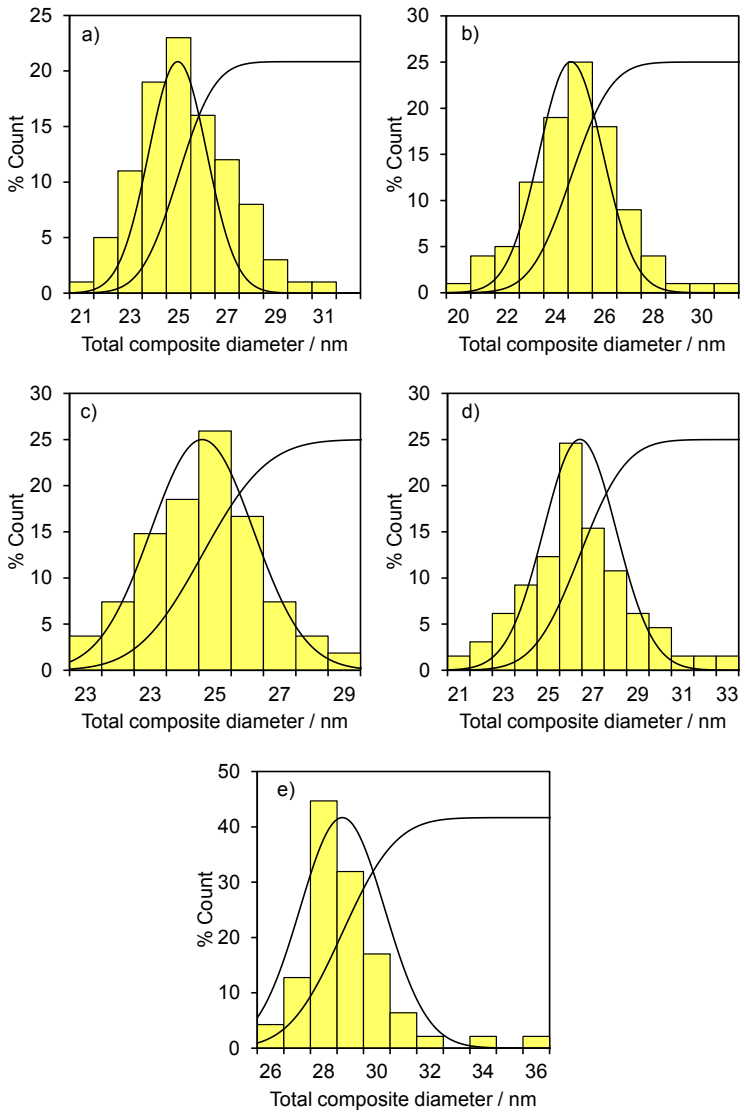

Fig, S4. Total nanocomposite size distributions, normal and cumulative size distributions of $Ag@SiO_2$ core-shell nanocomposites determined by HRTEM for a H value of 130 and W_o values of a) 2, b) 4, c) 6, d) 8 and e) 10.

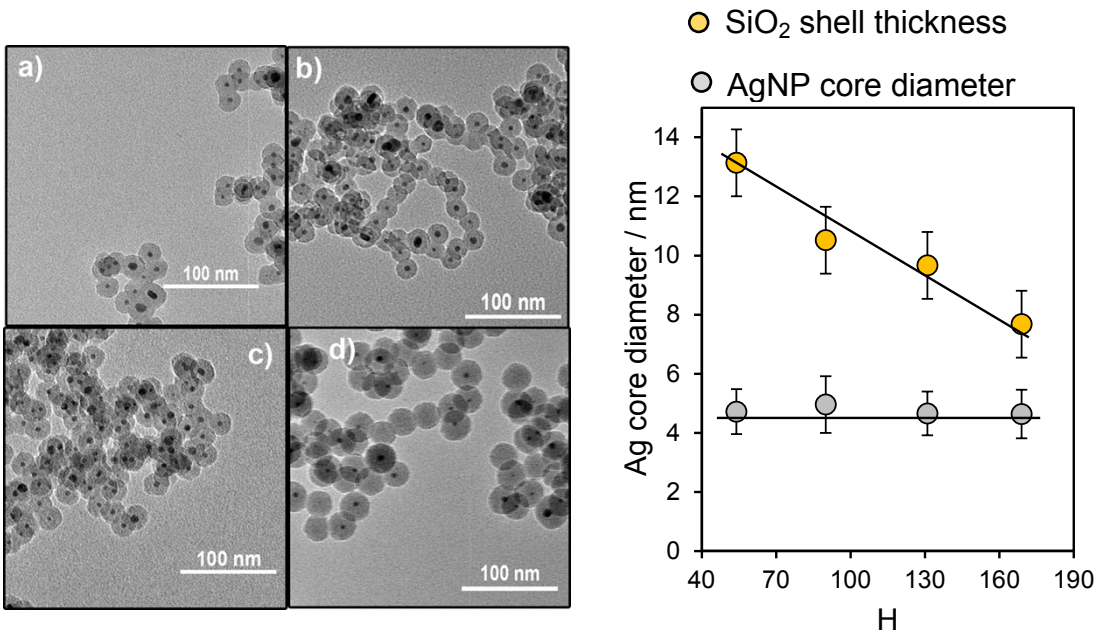

Fig. S5. (left) Representative HRTEM images of $Ag@SiO_2$ core-shell nanocomposites with a W_o value of 6 and H values of a) 170, b) 130, c) 90 and d) 55 and (right) Average AgNP particle sizes and SiO_2 shell thicknesses from HRTEM analysis images of $Ag@SiO_2$ core-shell nanocomposites with a W_o value of 6 as a function of H.

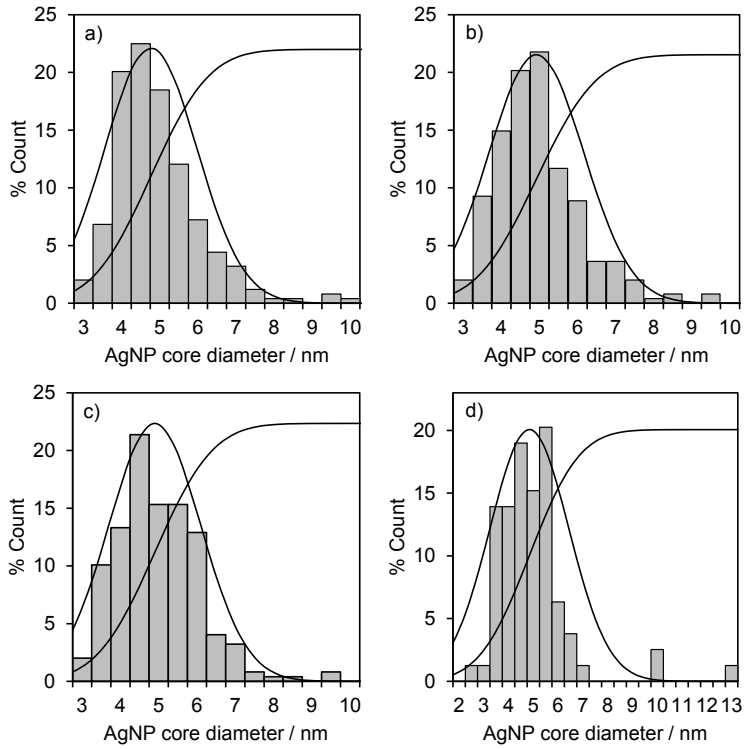

Fig. S6. Silver core size distributions, normal and cumulative size distributions of $Ag@SiO_2$ core-shell nanocomposites determined by HRTEM for $W_o = 6$ and H values of a) 170, b) 130, c) 90 and d) 55.

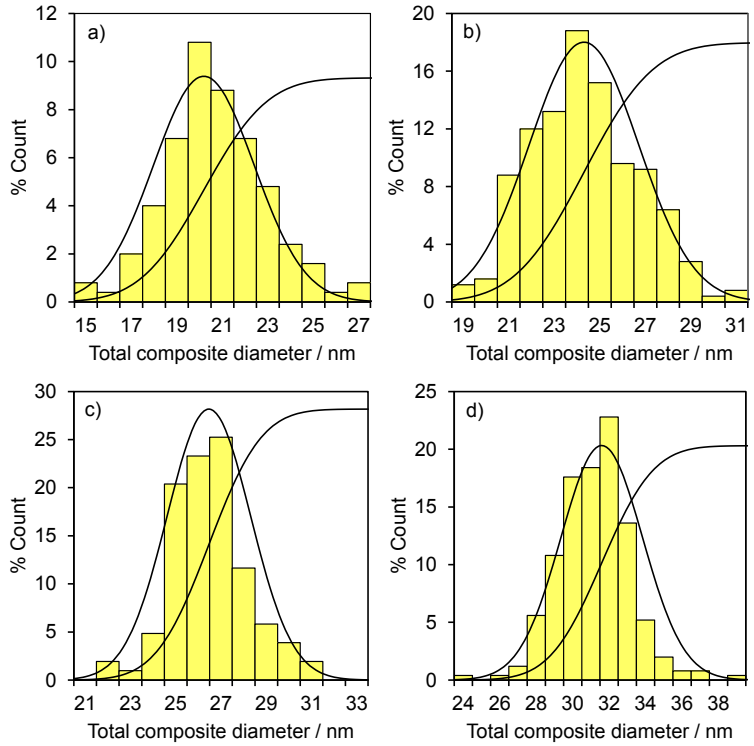

Fig. S7. Total nanocomposite size distributions, normal and cumulative distributions of $Ag@SiO_2$ core-shell nanocomposites determined by HRTEM for $W_o = 6$ and H values of a) 170, b) 130, c) 90 and d) 55.

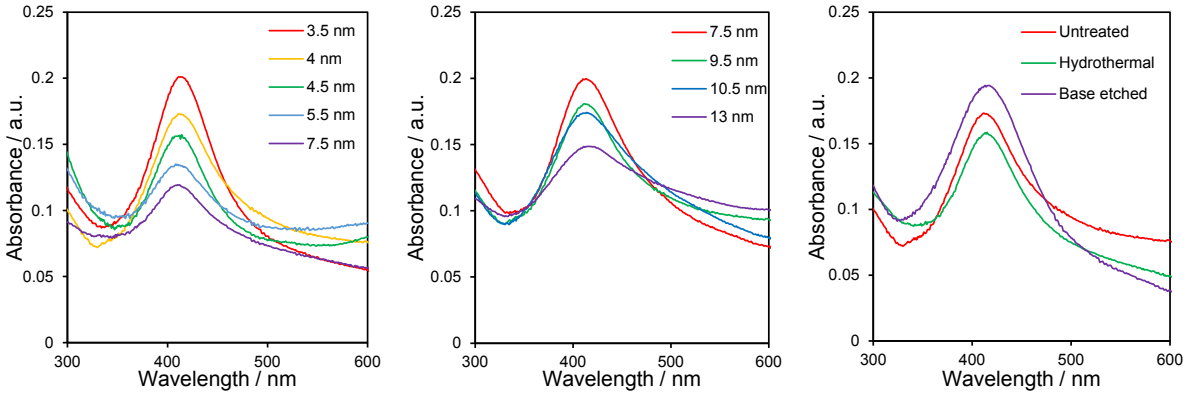

Fig. S8. UV-Vis spectra of (left) variable core size and constant shell thickness (9.5±1.2 nm, H = 130), (centre) variable total composite size and constant AgNP core size (4.5±0.4 nm, $W_o = 6$) and (right) constant AgNP core size (4.5±0.4nm, $W_o = 6$) and constant shell thickness (9.5±1.2 nm, H = 130) of various post synthetic treatments.

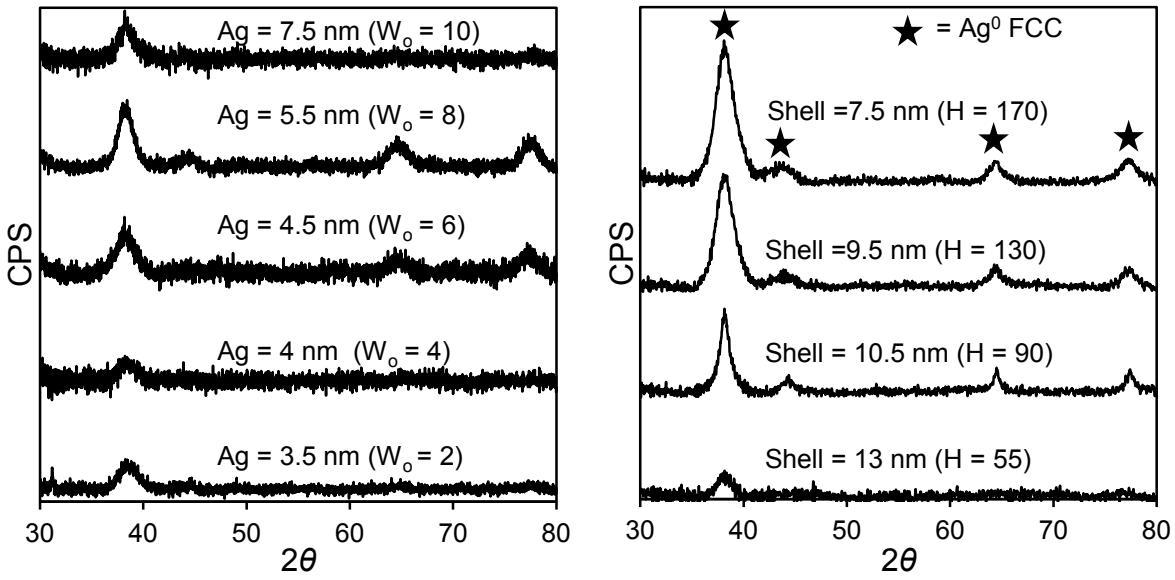

Fig. S9. Powder XRD patterns of Ag@SiO_2 core-shell nanocomposites of (left) variable core size and constant shell thickness (9.5±1.2 nm, H = 130) and (right) variable total composite size and constant AgNP core size (4.5±0.4 nm, W_o = 6).

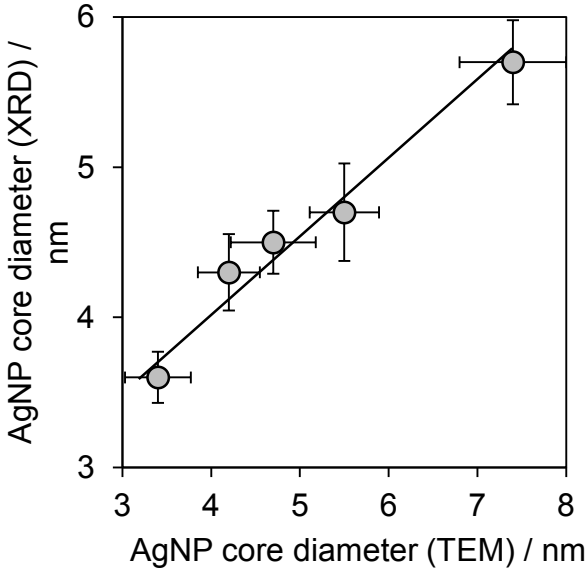

Fig. S10. Correlation between fcc Ag nanoparticle size of Ag@SiO_2 core-shell nanocomposites determined from XRD and HRTEM for Ag@SiO_2 as a function of W_o for H = 130 (shell thickness = 9.5±1.2 nm).

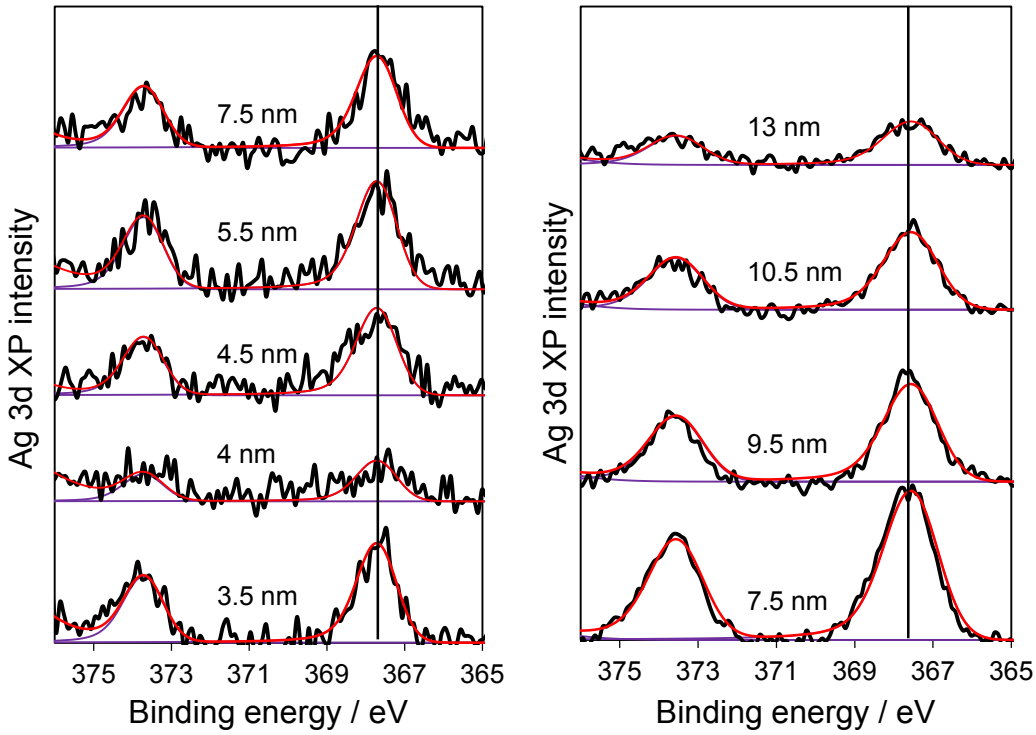

Fig. S11. Ag 3d XP spectra of Ag@SiO_2 core-shell nanocomposites for (left) variable core size and constant shell thickness (9.5±1.2 nm, H = 130) and (right) variable total composite size and constant AgNP core size (4.5±0.4 nm, W_o = 6).

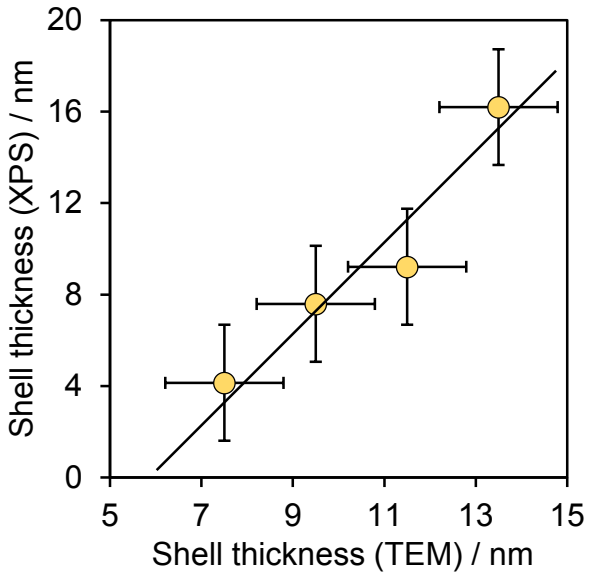

Fig. S12. Correlation between silica shell thickness of Ag@SiO_2 core-shell nanocomposites (possessing a common 4.5±0.4 nm diameter silver core) estimated from analysis of Ag 3d XP spectra using **Eq. S1** and HRTEM.

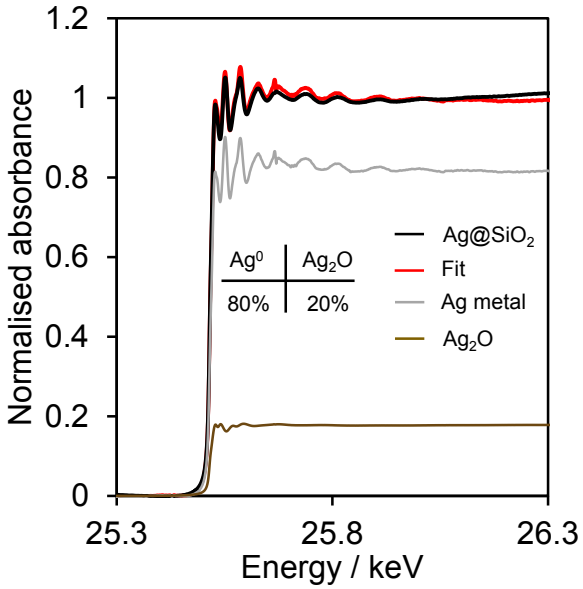

Fig. S13. Linear combination fitting of Ag K-edge XANES spectrum of $Ag@SiO_2$ core-shell nanocomposite possessing a 4.5±0.4nm diameter silver core and 9.5±1.2 nm thick SiO_2 shell to Ag foil and Ag_2O references.

The proportion of silver present in the nanocomposite as Ag^+ may be estimated geometrically by assuming that all silver atoms are present within the core (i.e. none dispersed throughout the silica shell), and that only silver atoms in the terminating surface of the core and hence direct contact with the silica shell are electron deficient. For this case, then the proportion of ionic silver within the core ($Ag^+ + Ag^0$) can be estimated from the equation below, using only the diameter of the silver core measured by HRTEM and ionic radius of Ag^+.

$$\% Ag^+ = V_{Ag+\ surface} / V_{core} * 100 = (V_{core} - V_{Ag0}) / V_{core} * 100 = (r_{core} - r_{Ag0})3 / r^3_{core} * 100 \quad \textbf{Eq. S1}$$

For a 5 nm diameter silver core (radius 2.5 nm)

Radius of Ag^0 core = 2.5 - Ag^+ ionic radius = 2.5 - 0.177 = 2.323 nm

Therefore,
$\% Ag^+ = (2.5-2.323)^3 / 2.5^3 * 100 = 3.1 / 15.625 =$ <u>19.8 %</u> in excellent agreement with **Fig. S12**.

Silver dissolution

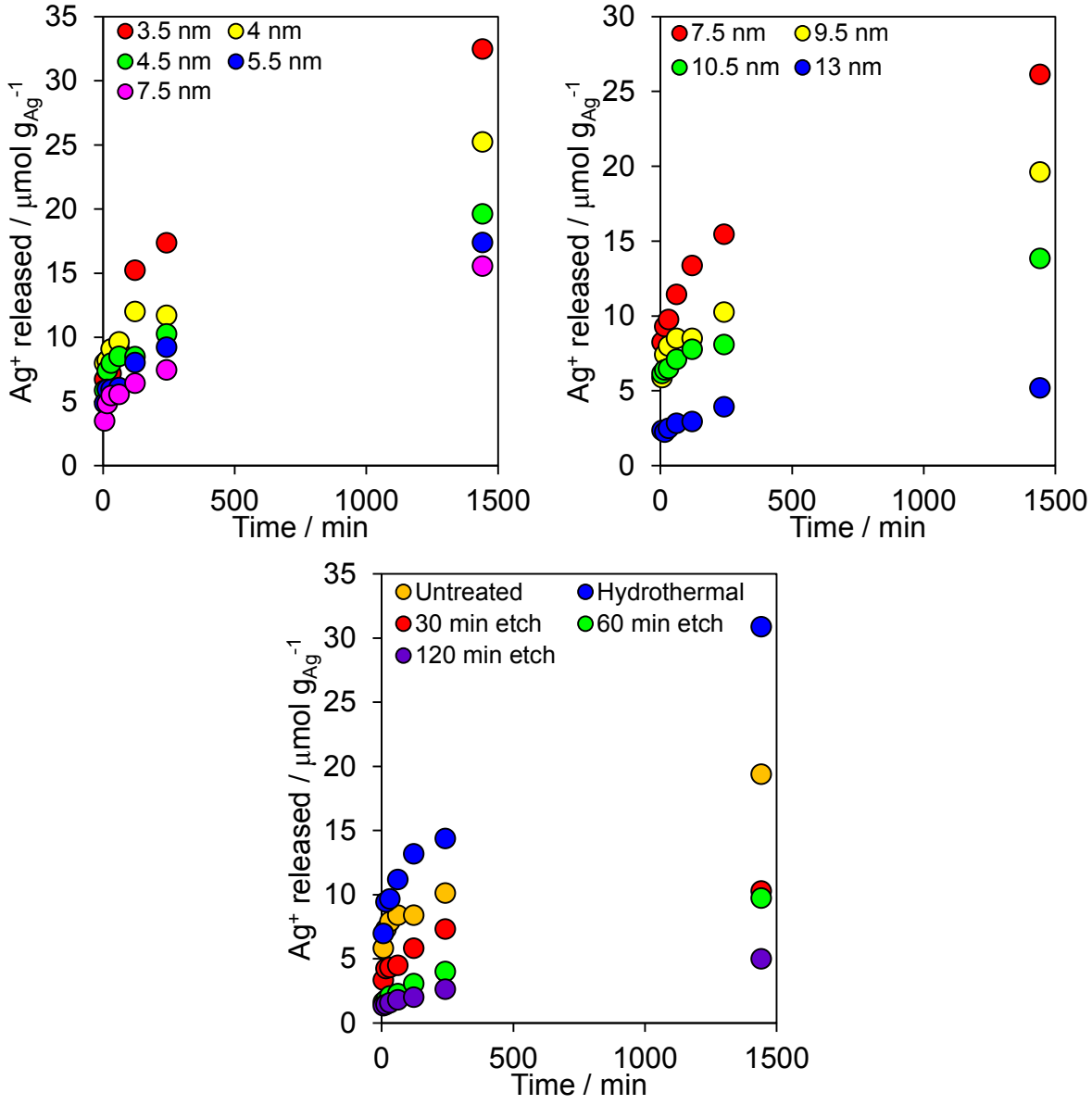

Fig. S14. Mass normalised Ag^+ dissolution profiles for a $Ag@SiO_2$ core-shell nanocomposite as a function of (top-left) silver core diameter for a fixed 9.5±1.2 nm SiO_2 shell thickness, (top-right) total composite size for fixed 4.5±0.4 nm silver core diameter, and (bottom) hydrothermal versus base etching treatment with 0.1 M NaOH.

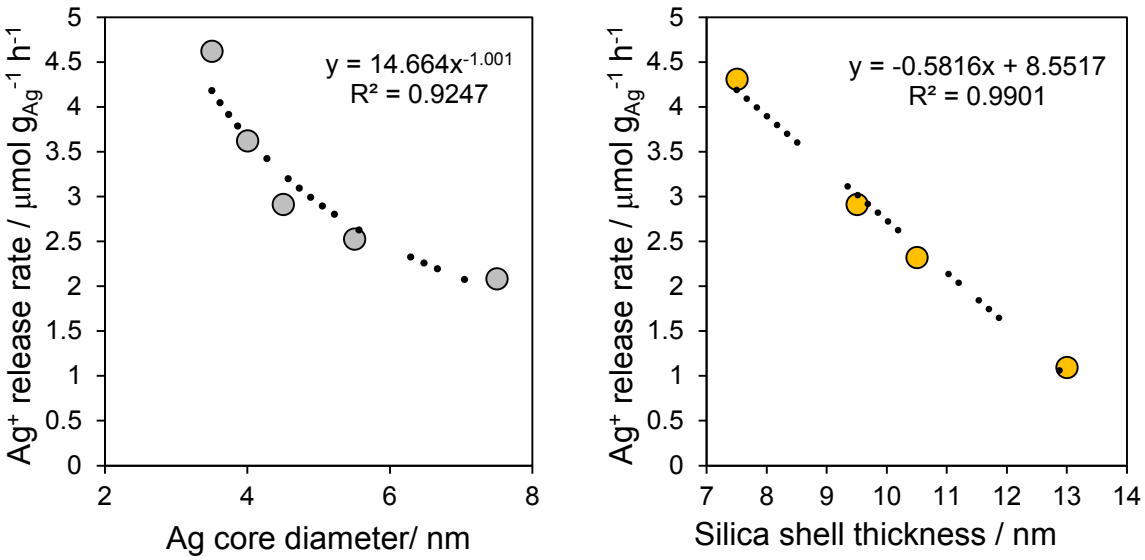

Fig. S15. Correlation between Ag^+ release rate and $Ag@SiO_2$ core-shell nanocomposite dimensions.

Nanocomposite etching

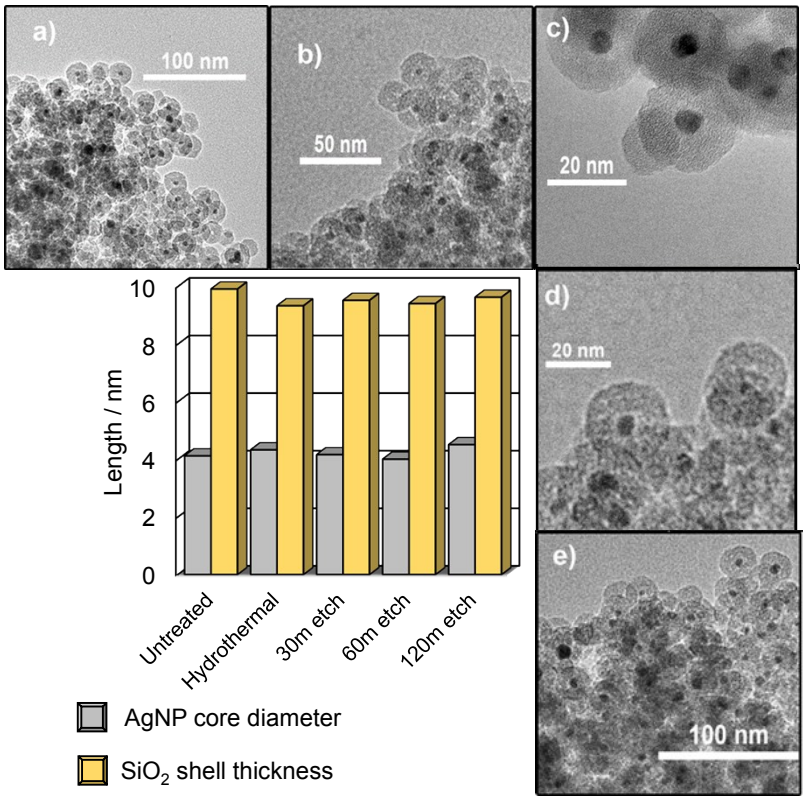

Fig. S16. HRTEM of $Ag@SiO_2$ core-shell nanocomposite possessing a 4.5±0.4 nm diameter silver core and 9.5±1.2 nm thick SiO_2 shell (a) as-prepared, (b) after hydrothermal treatment, and after (c) 30 min (d) 60 min and (e) 120 min etching treatment with 0.1M NaOH.

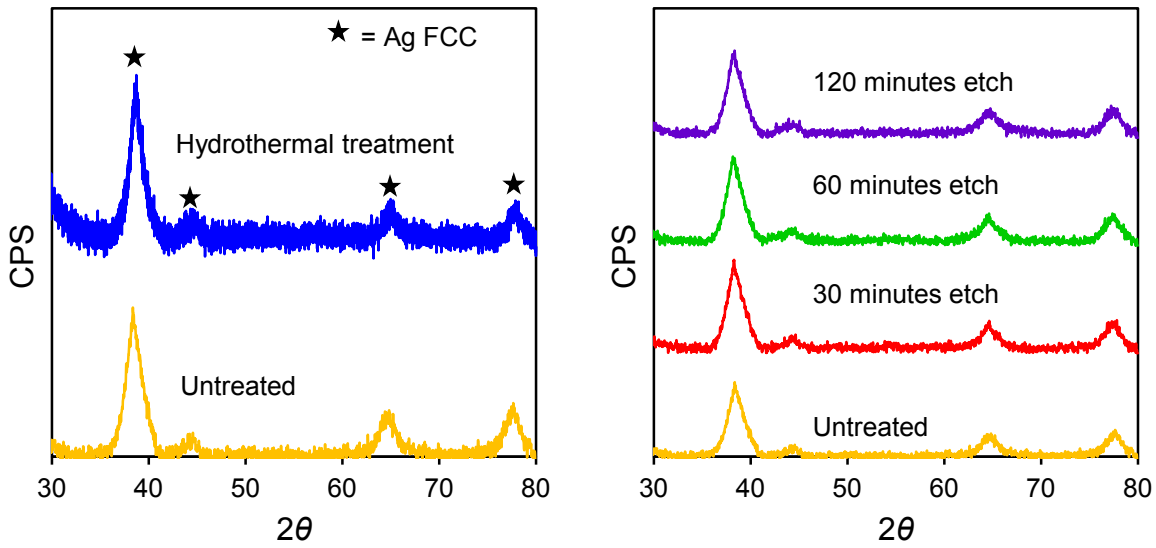

Fig. S17. Powder XRD pattern of Ag@SiO_2 core-shell nanocomposite possessing a 4.5±0.4 nm diameter silver core and 9.5±1.2 nm thick SiO_2 shell (a) as-prepared, (b) after hydrothermal treatment, and after (c) 30 min (d) 60 min and (e) 120 min etching treatment with 0.1 M NaOH.

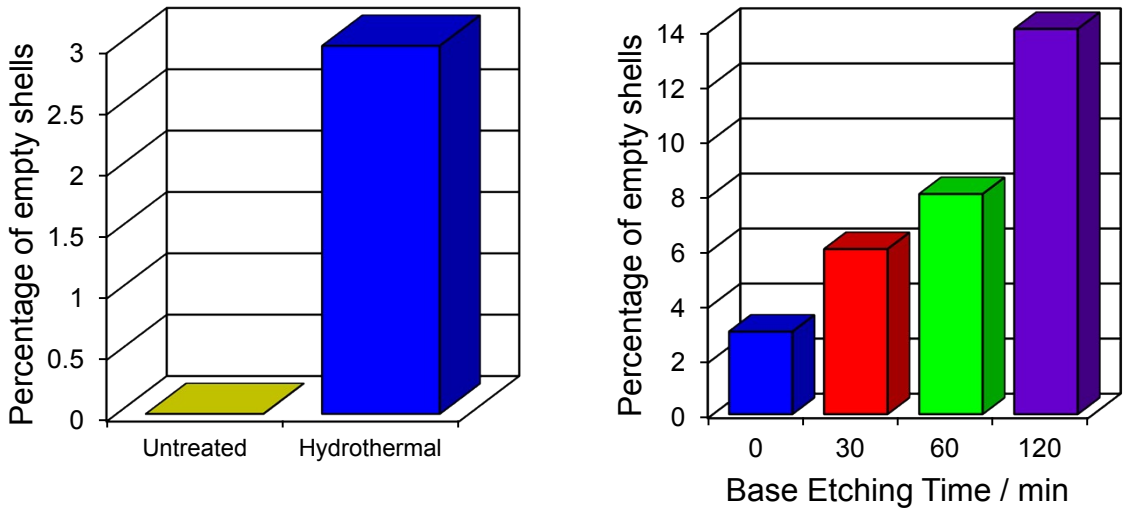

Fig. S18. Percentage of Ag core loss from a Ag@SiO_2 core-shell nanocomposite possessing a 4.5±0.4 nm diameter silver core and 9.5±1.2 nm thick SiO_2 shell as a function of (left) hydrothermal treatment and (right) hydrothermal (0 min) versus base etching treatment with 0.1 M NaOH.

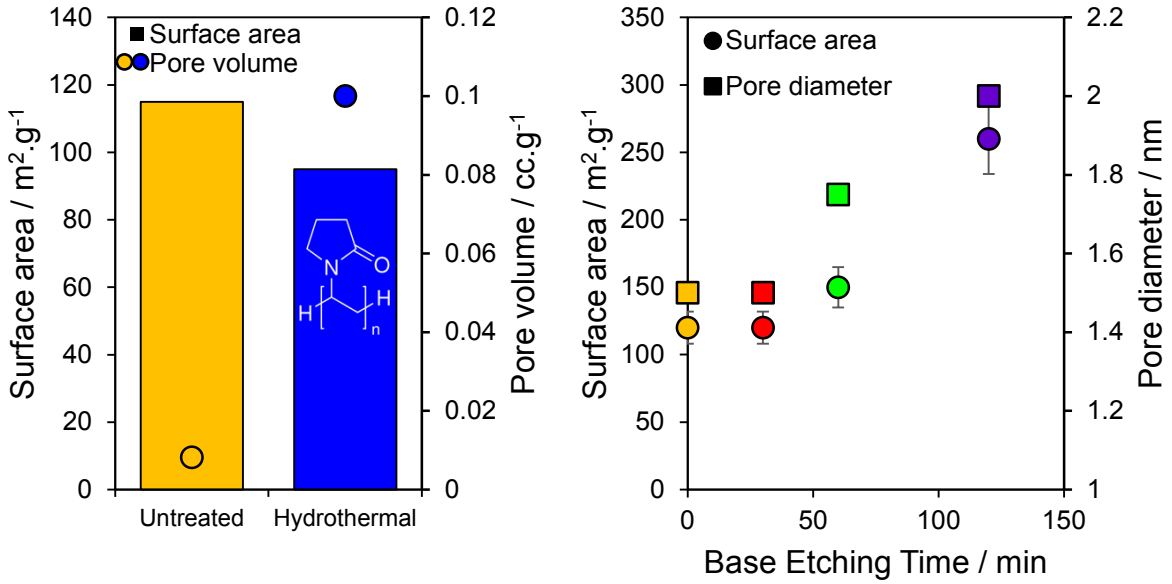

Fig. S19. Change in BET surface area of a Ag@SiO_2 core-shell nanocomposite possessing a 4.5±0.4n m diameter silver core and 9.5±1.2 nm thick SiO_2 shell following hydrothermal or etching treatment with 0.1 M NaOH.

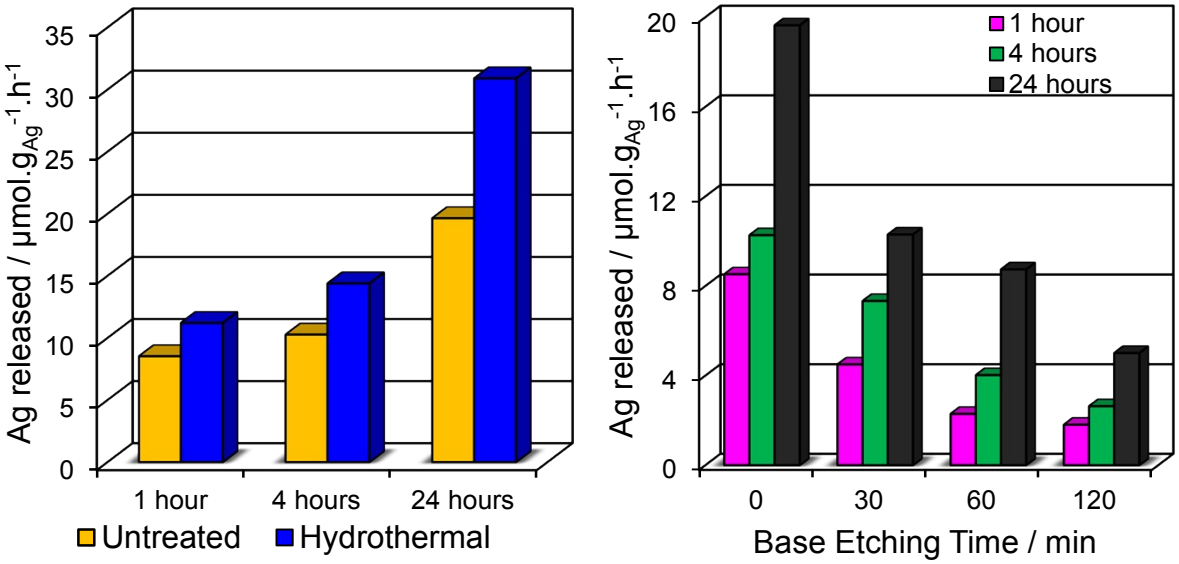

Fig. S20. Total Ag^+ released from Ag@SiO_2 core-shell nanocomposites possessing a 4.5±0.4 nm diameter silver core and 9.5±1.2 nm thick SiO_2 shell following (left) hydrothermal, and (right) base etching treatments.

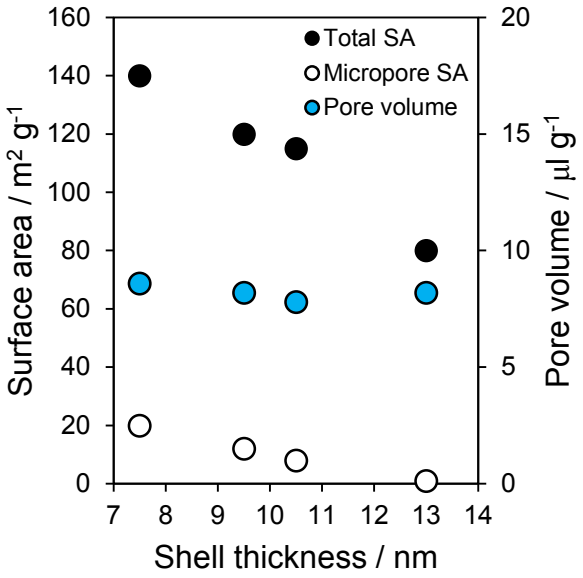

Fig. S21. Surface area, pore volumes and micropore surface areas of Ag@SiO_2 core-shell nanocomposites as a function of total composite diameter for a fixed 4.5±0.4 nm silver core diameter.

.

$$2\,Ag_{(s)} + {}^{1}/_{2}O_{2(aq)} + 2H^{+}_{(aq)} \longrightarrow 2\,Ag^{+}_{(aq)} + H_2O_{(l)}$$

Scheme S1. Oxidative dissolution of silver.

Antimicrobial testing

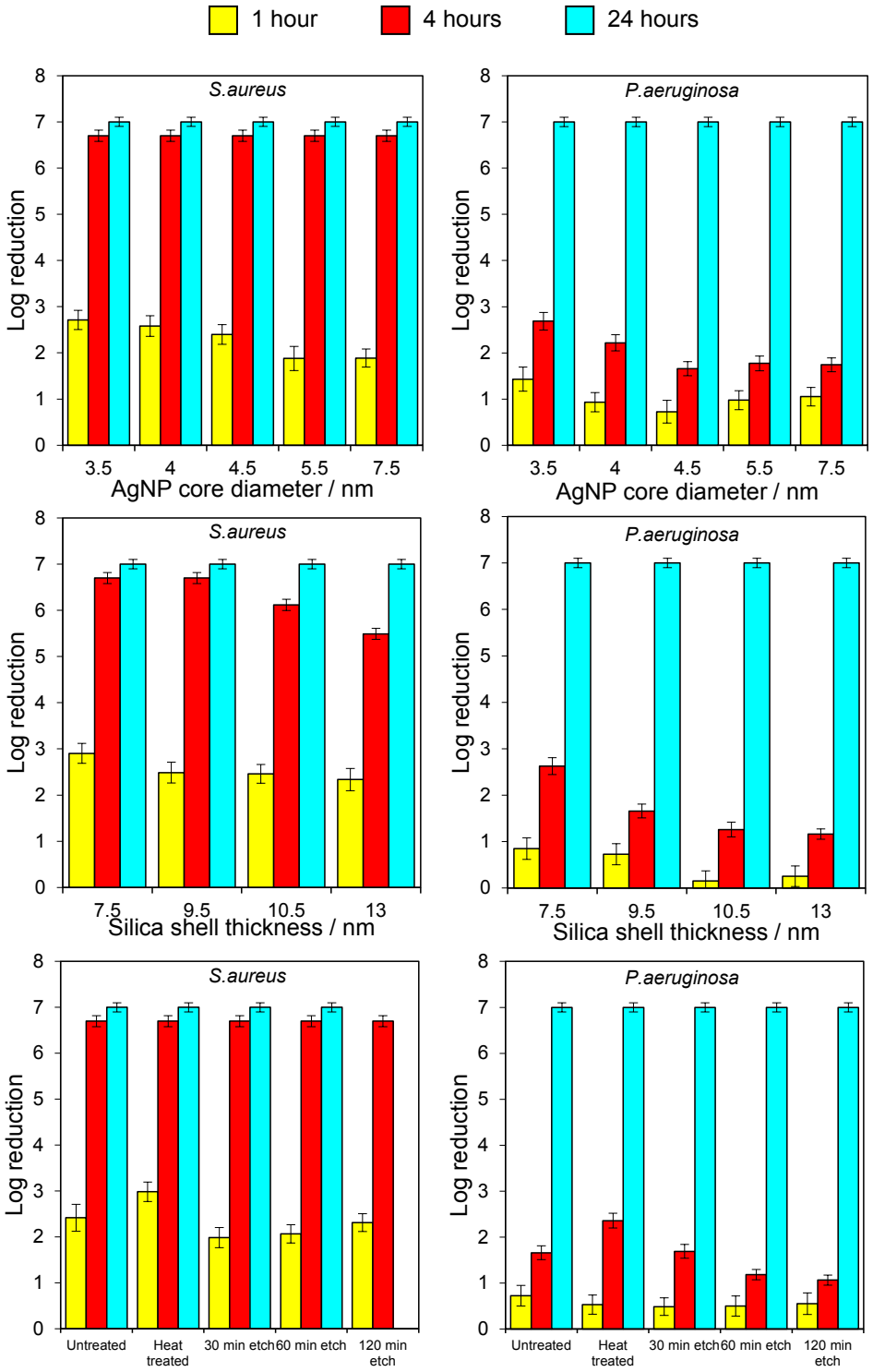

Fig. S22. Logarithmic reduction for Ag@SiO_2 core-shell nanocomposites tested against *Staphylococcus aureus* ATCC 6538 and *Pseudomonas aeruginosa* ATCC 15442 as a function of (top) silver core diameter for a fixed 9.5±1.2 nm SiO_2 shell thickness, (middle) silica shell thickness for a fixed 4.5±0.4 nm silver core diameter, and (bottom) etching protocol for a nanocomposite possessing a 4.5±0.4 nm diameter silver core and 9.5±1.2 nm thick SiO_2 shell.